JOURNAL OF MATERIALS SCIENCE 24 (1989) 3892–3903

The preparation and properties of some lithium zinc silicate glass-ceramics

I. W. DONALD*, B. L. METCALFE*, D. J. WOOD‡ and J. R. COPLEY§
*Atomic Weapons Establishment, Aldermaston, Berkshire, UK
‡School of Materials Science and Physics, Thames Polytechnic, London, UK
§School of Chemical Physics, University of Bristol, Bristol, UK

Lithium zinc silicate glasses are of interest for the preparation of moderately high thermal expansion glass-ceramics which are suitable for sealing to a number of nickel-based superalloys. The effect of composition, in particular the variation of nucleating species, on the crystallization behaviour of a number of these glasses has been examined using differential thermal analysis, X-ray diffraction, and electron microscopy. Various crystal phases have been identified, including cristobalite, quartz, tridymite and γ_0 Li_2ZnSiO_4. In addition, most of the glass-ceramics also contain an unidentified phase which may be related to the β-series of lithium zinc silicates. Heat-treatment schedules have been derived on the basis of these results in order to produce a number of glass-ceramic materials. The resultant thermal expansion characteristics of the glass-ceramics have been monitored using dilatometry, and expansions in the range ≈ 12.3 to $17.1 \times 10^{-6}\,^{\circ}C^{-1}$ (20 to 460° C), have been obtained, depending on the precise glass composition and heat-treatment schedule employed. In addition, the mechanical properties of a number of selected samples have been monitored, employing a biaxial flexure technique.

1. Introduction

One of the most important applications of oxide glasses has been as electrical insulating components for use in a variety of electrical and electronic devices. Early vacuum tubes relied heavily on the property of certain glasses to bond well to metals, so forming strong hermetic seals and, in addition, electrically isolating the metallic components from one another (e.g. [1]). Later, McMillan and coworkers [2–4] showed that glass-ceramics could also be employed to produce superior glass-ceramic-to-metal seals. Glass-ceramics offer the advantages of glass-to-metal seals, in particular ease of fabrication, including relatively low sealing temperatures, in addition to several other important advantages. These include higher mechanical strength and more refractory behaviour, relative to their glassy counterparts, coupled with the ability to tailor the thermal expansion characteristics to match those of almost any metal or alloy. Despite the versatility of glass-ceramics, however, wide scale commercial exploitation has been relatively limited (e.g. [5–12]). This is particularly true for ceramic-to-metal seal applications, although there has been a moderate increase in interest over the last few years (e.g. [13–18]).

In the UK, a recent study required the development of a glass-ceramic for sealing to nickel-based superalloys, and it was shown that materials from the Li_2O–ZnO–SiO_2 system appeared particularly promising [19]. Lithium zinc silicate glass-ceramics containing high proportions of zinc oxide were first reported by McMillan and Partridge in 1963 [20], and further work was published in the period up until 1967 [3, 4, 21–26]. With a few notable exceptions, however, (e.g. [27–29]) very little detailed work has since been reported on this system, particularly in connection with the development of suitable materials with practical applications.

In the present paper, we describe and discuss work carried out on a number of Li_2O–ZnO–SiO_2 materials containing relatively high concentrations of ZnO. This comprises a study of the crystallization behaviour of selected glasses, including the influence of nucleating species and concentration, and an assessment of the thermal expansion characteristics and mechanical properties of some of the resultant glass-ceramics.

2. Experimental procedures

2.1. Preparation of glass samples

Glass batch materials were prepared, using the constituents summarized in Table I, by tumbling the appropriate powders, calculated to yield 500 g samples of glass, for 1 h in polyethylene bottles. The batches were then melted in air in a closed Pt–5% Rh crucible at a maximum temperature of 1500° C for 3 to 5 h. Good homogeneity was achieved by quenching the molten glass in de-ionized water, which produced a granulated product, followed by remixing and remelting of the product, this procedure being carried out at least twice. Details of the glass compositions prepared are given in Table II. These are nominal

0022–2461/89 $03.00 + .12

TABLE I Glass batch constituents

1.	Li_2O – BDH, GPR Li_2CO_3
2.	Na_2O – BDH, GPR anhydrous Na_2CO_3
3.	K_2O – BDH, AR K_2CO_3
4.	ZnO – BDH, AR ZnO
5.	B_2O_3 – M & B Laboratory Chemicals H_3BO_3, and/or BDH, AR $Na_2B_4O_7 . 10H_2O$
6.	Al_2O_3 – BDH, AR Al_2O_3
7.	P_2O_5 – BDH, AR anhydrous Na_2HPO_4, and/or BDH, GPR $Zn_3(PO_4)_2 . 4H_2O$
8.	MoO_3 – BDH, AR MoO_3
9.	CuO – Koch-Light, pure CuO
10.	SiO_2 – Tilcon L3OA low-iron silica sand

compositions; weight losses during melting were generally less than 0.5 wt %.

Molten glass was subsequently cast into preheated (to 450° C) graphite moulds of 38 mm internal diameter to give solid cylinders of glass approximately 80 mm in height. These cylinders were immediately annealed for 1 h, and then furnace-cooled at $\approx 0.5°\,C\,min^{-1}$ to room temperature. The annealing temperature for each glass composition employed was based on prior knowledge of the glass transition temperature, T_g, as determined by differential thermal analysis employing a Stanton Redcroft DTA Model 674, operating at a heating rate of $10°\,C\,min^{-1}$. Samples of glass rod 6 or 8 mm in diameter were also prepared by casting into suitable graphite moulds, annealing subsequently being carried out as described above.

Samples of glass rods about 6 mm in diameter of compositions B and C were also provided by Sandia National Laboratories, Alberquerque, USA (SNLA). These glasses were prepared by melting at a lower temperature (1275° C) whilst stirring the melt in order to achieve good homogeneity. Batches of glasses B and C prepared in our own laboratory and at SNLA were subsequently chemically analysed for comparison. These analysed compositions are given in Table III, and are seen to compare very favourably, despite the different preparation techniques.

2.2. Conversion of glass to glass-ceramic

The glass cylinders were cut into suitably sized samples using a diamond wheel, and cleaned in order to remove all surface contaminants which may give rise to preferential surface crystallization during heat-treatment. The following cleaning procedure was adopted. The samples were first rinsed in acetone; they were then ultrasonically cleaned in dichloroethane, followed by further ultrasonic cleaning in isopropanol; finally, they were dried under an infrared lamp. Samples were then heat-treated under a variety of conditions, employing a Wentgate Model 0810 vacuum furnace, modified to operate under a positive pressure of argon. For most of the work, a simulated sealing cycle was performed in addition to nucleation and crystallization heat-treatment cycles, as depicted in Fig. 1.

2.3. Measurement of thermal properties

The thermal properties of the glasses, in the form of as-quenched powder, were monitored using the Stanton Redcroft Differential Thermal Analyser. The DTA was calibrated over a range of temperatures and heating rates using standard materials (K_2SO_4 and Ag_2SO_4). It was noted that heating rate, $\dot{T}$, corrections only became significant for $\dot{T} > 15°\,C\,min^{-1}$. All work was therefore confined to $\dot{T} < 15°\,C\,min^{-1}$, with the majority of work being performed at a standard heating rate of $10°\,C\,min^{-1}$.

A preliminary assessment of the efficiency of a given nucleating agent or additive was made using the method of Thakur and Thiagarajan [30], in which the variation in peak crystallization temperature with particle size is monitored. Two size fractions were used in the present work, a fine sample 0 to 212 μm in size, and a coarse sample 600 to 1000 μm. Optimum nucleating temperatures were also measured using the method of Marotta *et al.* [31–34]. In this technique, the optimum nucleation temperature is found by plotting the difference in peak crystallization temperature between as-quenched and nucleated glass samples against the temperature of nucleation. The method offers a very simple and relatively quick way of finding optimum nucleation temperatures for different glasses, involving the use of DTA only. In the present work, a standard glass particle size of 600 to 1000 μm was employed, and samples were nucleated *in situ* in the DTA for 1 h in the temperature range 400 to 620° C. Peak crystallization temperatures were then monitored by heating the samples through the crystallization range at $10°\,C\,min^{-1}$. Optimum nucleating times were assessed by holding at the optimum nucleating temperature, as determined by the above method, for various periods of time, the procedure again being carried out in the DTA.

Apparent activation energies for crystallization were determined following the modified Kissinger method, as described by Matusita *et al.* [35–37]. This technique makes use of the relationship

$$\ln (\dot{T}^n/T_p^2) = -(mE/RT_p) + \text{constant} \quad (1)$$

TABLE II Nominal compositions of glasses employed in present work (mol %)

Glass code	Li_2O	Na_2O	K_2O	ZnO	B_2O_3	Al_2O_3	MoO_3	CuO	P_2O_5	SiO_2
A	18.19	4.87	–	18.11	4.34	–	–	–	–	54.54
B	18.01	4.82	–	17.93	4.29	–	–	–	1.01	53.94
C	17.96	4.80	–	17.87	4.28	–	–	–	1.31	53.78
D	17.89	4.79	–	17.81	4.26	–	–	–	1.65	53.60
E	17.75	4.75	–	17.67	4.22	–	–	1.14	1.32	53.15
F	17.91	1.47	1.61	17.82	4.26	0.60	–	–	1.33	55.00
G	18.01	4.82	–	17.93	4.29	–	1.00	–	–	53.95

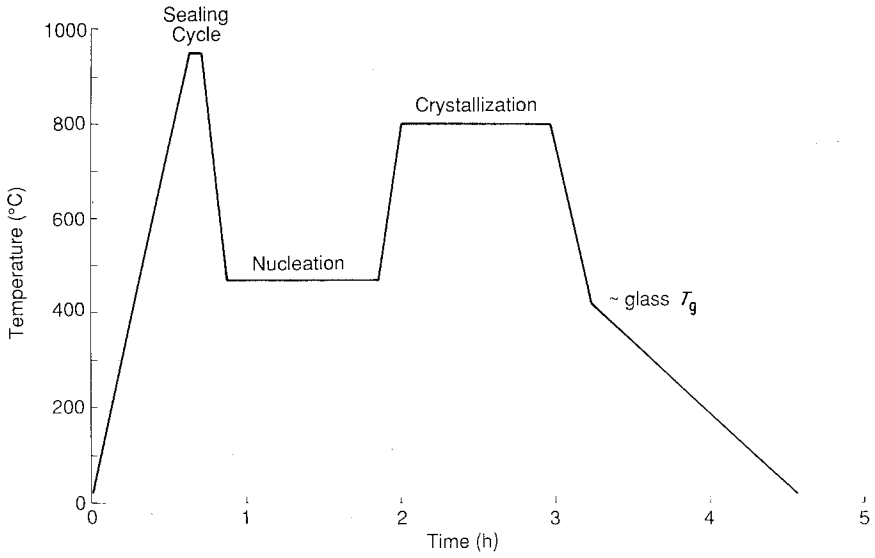

Figure 1 Representative sealing and heat-treatment cycles.

where T_p is the crystallization peak temperature, E the activation energy, R the gas constant and n and m are numerical factors which depend on the crystallization mechanism.

In this method, $\ln(\dot{T}^n/T_p^2)$ is plotted against $1/T_p$, and E is found from the slope of the resulting graph. The method requires a prior knowledge of the crystallization mechanism in order to assign the appropriate values to n and m. For example, for $n = m = 1$, surface crystallization would normally predominate, whilst for $n = m = 3$, three-dimensional bulk crystallization from a constant number of nuclei predominates [35–37]. In the present work, samples were nucleated for 2 h at the optimum nucleation temperature, and values of $n = m = 3$ were used. Apparent activation energies for crystallization were also found for some of the samples which had not been subjected to a separate nucleation stage. In these cases, values of $n = 4$ and $m = 3$ were employed, corresponding to bulk crystallization from an increasing number of nuclei, N, i.e. $N \propto 1/\dot{T}$.

2.4. Thermal expansion characteristics

The thermal expansion characteristics of the materials in the form of rod 6 or 8 mm in diameter were monitored at a heating rate of 5° C min^{-1} using a dilatometer supplied by Ceramic Developments (Midlands) Ltd. This was of the single push-rod variety employing a linear variable differential transformer, LVDT, and with an operating capability in air from ambient to 1000° C.

2.5. X-ray diffraction

As-cast and heat treated samples were examined using a Philips PW1710 diffractometer employing Cu Kα radiation from $2\theta = 5$ to 100°.

TABLE III Chemically analysed glass compositions (mol %)

Glass code	Li_2O	Na_2O	ZnO	B_2O_3	P_2O_5	SiO_2
B-UK	18.74	4.81	18.67	3.51	0.92	53.35
B-US	18.03	4.73	19.49	3.01	0.84	53.89
C-UK	18.11	4.85	18.91	3.54	1.27	53.33
C-US	18.07	4.65	19.17	3.02	1.10	54.01

UK glasses prepared by present authors.
US glasses prepared at SNLA.

2.6. Microstructure

Microstructures were examined by optical and scanning electron microscopy (SEM), after polishing samples and then etching for a few seconds in an aqueous solution of 0.5% HF + 0.5% H_2SO_4. SEM samples were coated with Au–Pd alloy prior to examination.

2.7. Mechanical properties

Disc samples of about 1.4 mm in thickness were cut from the as-cast and heat-treated materials using a diamond wheel. The discs were given no further treatment, the cutting process yielding a standard abrasion treatment. Samples were then tested in biaxial flexure, using a loading rate of 0.75 mm min^{-1}. The piston-on-three-ball method was employed in which a glass or glass-ceramic sample in the form of a thin disc is supported on three equi-spaced ball bearings situated on a circle of diameter d, and a piston is used to transmit load to the central region of the disc [38–41]. In the present work, 38 mm diameter discs were tested using a piston diameter of 2.4 mm, and for $d = 25.4$ mm. This method, which offers the advantage that the fracture stress is independent of the condition of the edges of the sample, requires a knowledge of Poisson's ratio for the material tested; a standard value of 0.24 was taken for all the materials investigated in this work.

3. Results

3.1. Thermal properties of glasses

3.1.1. Differential thermal analysis investigations

The thermal properties of the glasses, designated compositions A to G, are given in Table IV. The composition which contains no specific nucleating agent (A) exhibits only a broad, diffuse crystallization exotherm. On the other hand, compositions that contain P_2O_5 (B to D), exhibit two well resolved crystallization peaks, the separation between the peaks and the sharpness of the peaks increasing as the

concentration of P_2O_5 increases; the increase in peak separation is a result of the first crystallization peak being shifted to lower temperatures, there being no significant change in the temperature of the second peak. The composition which contains Al_2O_3 in addition to P_2O_5 (F) exhibits not only a shift to lower temperatures of the first crystallization peak, but also a shift in the second peak to a higher temperature. The glass which contains 1.00 mol % MoO_3 as nucleating agent (G) also exhibits two crystallization peaks with similar peak temperatures to those obtained with 1.31 mol % P_2O_5. All the glasses show well defined T_gs and melting ranges. Representative DTA traces are shown in Fig. 2.

Nucleating efficiencies, as determined by the variation in peak temperature between coarse and fine samples of glass powder, are summarized in Table V. The data for finding the optimum nucleating temperature of a given glass, in which the difference in peak temperature between as-quenched and nucleated glasses is plotted against the nucleating temperature employed, are shown in Fig. 3a and the data for finding the optimum time are shown in Fig. 3b. A typical DTA trace which illustrates the shift in crystallization peaks effected by nucleation is shown in Fig. 4. Activation energies for crystallization, as determined by DTA, are given in Table VI . A representative plot of $\ln \dot{T}^3/T_p^2$ against $1/T_p$ for sample B is shown in Fig. 5.

3.1.2. Thermal expansion characteristics

The thermal expansion of the lithium zinc silicate glasses studied is approximately $9.0 \times 10^{-6}\,°C^{-1}$ (20 to 460° C), irrespective of the precise composition. The expansion behaviour noted (Fig. 6) is similar to that which is observed for many inorganic glasses. Very characteristic expansion behaviour is found for the glass-ceramics, as also illustrated in Fig 6. A region of moderate expansion is noted between ambient and about 150° C. This is followed by a rapid increase in expansion over the range ≈ 150 to 240° C followed by a second region of moderate expansion behaviour up to about 520° C. A very high expansion regime is then encountered up to the maximum temperature investigated (≈ 650° C). The values of expansion noted for the glass-ceramics are very dependent on the composition and heat-treatment schedule, as summarized in Fig. 7.

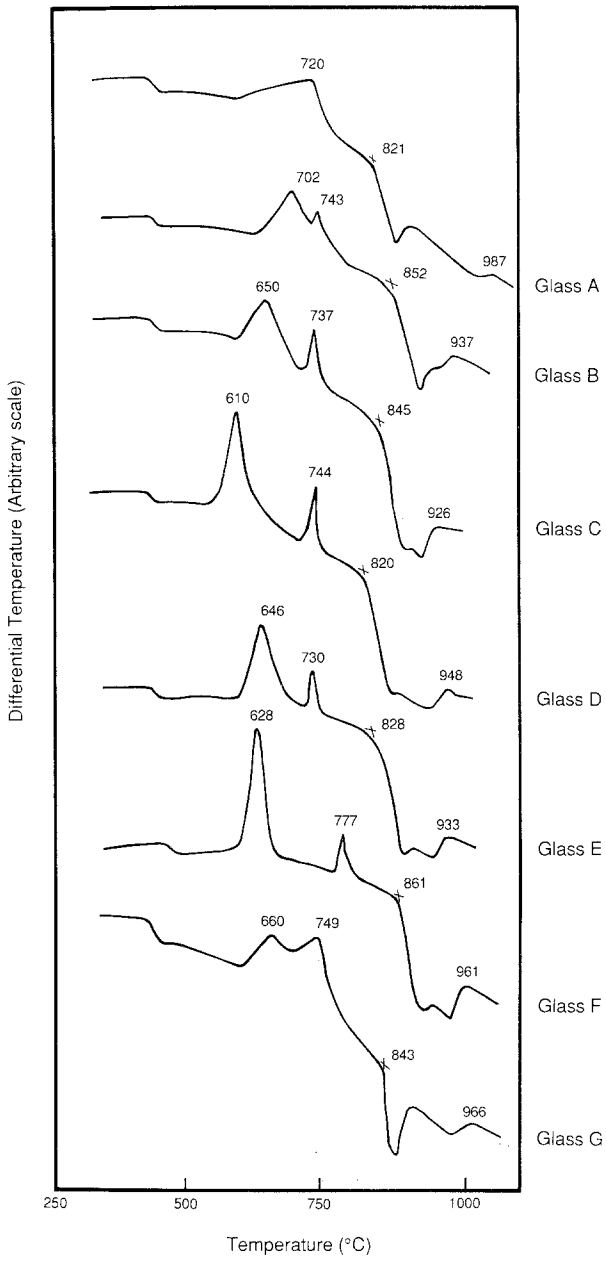

Figure 2 Typical DTA traces of as-quenched lithium zinc silicate glasses.

Fig. 7 shows the expansion coefficients of the glass-ceramics as a function of the (1 h) crystallization temperature for the temperature regime 20 to 460° C. In Fig. 7a, data for composition B are given for samples which have been heated to 950° C for 5 min (representing the sealing condition, see Fig. 1), followed

TABLE IV Thermal properties of glasses

Glass code	T_g (° C)	T_{xp1} (° C)	T_{xp2} (° C)	T_{ms} (° C)	T_{liq} (° C)
A	455 ± 1	≈ 720	–	821 ± 13	987 ± 6
B	459 ± 4	702 ± 8	743 ± 7	852 ± 16	937 ± 3
C	459 ± 3	650 ± 9	737 ± 5	845 ± 9	926 ± 6
D	464 ± 3	610 ± 5	744 ± 6	820 ± 8	948 ± 10
E	459 ± 1	646 ± 2	730 ± 4	828 ± 14	933 ± 5
F	472 ± 5	628 ± 6	777 ± 6	861 ± 11	961 ± 2
G	460 ± 1	660 ± 1	749 ± 1	843 ± 6	966 ± 2

T_g glass transition temperature
T_{xp1} temperature corresponding to first crystallization peak
T_{xp2} temperature corresponding to second crystallization peak
T_{ms} temperature corresponding to start of melting (see Fig. 2)
T_{liq} liquidus temperature (end of melting)

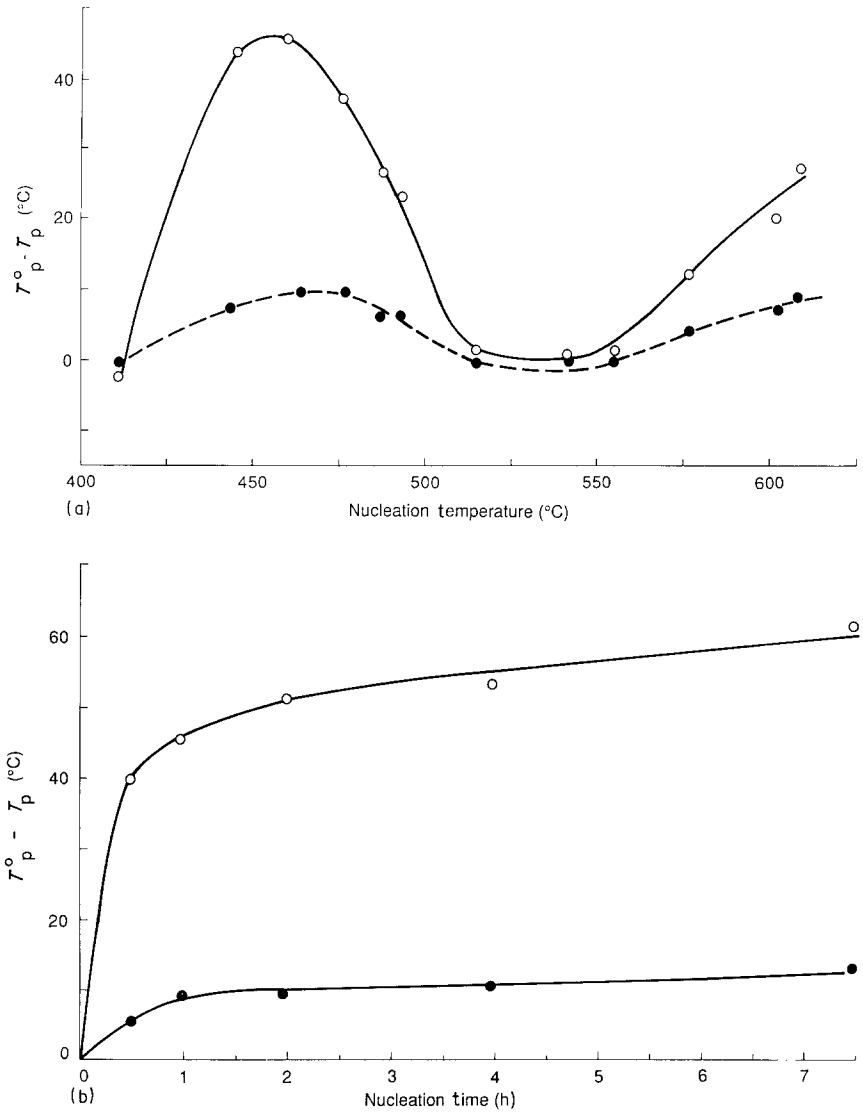

Figure 3 (a) Variation in peak temperature between as-quenched and nucleated glass (composition B) with temperature of nucleation — samples nucleated *in situ* in the DTA for 1 h. (b) Variation in peak temperature of as-quenched and nucleated glass (composition B) with time of nucleation at 465° C.

TABLE V Effect of small concentrations of additives on nucleating efficiency

Glass code	Additive (mol %)	Nucleation treatment	ΔT_{xp1} (° C)	ΔT_{xp2} (° C)
A	none	none	62	–
B	1.01 P_2O_5	none	23	6
B	1.01 P_2O_5	2 h at 465° C	0	0
C	1.31 P_2O_5	none	0	1
D	1.65 P_2O_5	none	0	9
E	1.31 P_2O_5 + 1.14 CuO	none	3	8
F	1.31 P_2O_5 + 0.60 Al_2O_3 + K_2O substitution	none	0	1
G	1.00 MoO_3	none	12	42
G	1.00 MoO_3	2 h at 465° C	16	37

TABLE VI Activation energies for crystallization

Glass code	Nucleation treatment	Activation energy (± 10 kJ mol^{-1})	
		First crystallization peak	Second crystallization peak
B	none	273	361
B	2 h at 465° C	256	280
C	none	306	384
C	2 h at 465° C	290	320
D	2 h at 465° C	312	343
F	2 h at 465° C	344	323

TABLE VII Summary of X-ray diffraction data

Glass code	Heat-treatment schedule Temp (°C) / time (min)	Crystal phases identified
B	as-cast	Amorphous
B	950/5 + 465/60 + 700/60	α-crist + unknown LZS
B	950/5 + 465/60 + 750/60	α-crist + unknown LZS
B	950/5 + 465/60 + 800/60	α-crist + quartz + unknown LZS
B	950/5 + 465/60 + 850/60	α-crist + tridymite? + unknown LZS
B	950/5 + 465/60 + 850/60*	Tridymite + γ_o LZS
C	as-cast	Amorphous
C	950/5 + 465/60 + 700/60	α-crist + quartz + unknown LZS
C	950/5 + 465/60 + 700/60†	α-crist + unknown LZS
C	950/5 + 465/60 + 750/60†	α-crist + unknown LZS
C	950/5 + 465/60 + 800/60†	α-crist + tridymite + unknown LZS
C	950/5 + 465/60 + 850/60	α-crist + quartz + unknown LZS
C	950/5 + 465/60 + 850/60†	α-crist + tridymite + unknown LZS
C	465/60 + 650/60*	Amorphous + α-crist + unknown LZS
C	465/60 + 700/60*	α-crist + unknown LZS
C	465/60 + 800/60*	α-crist + quartz + unknown LZS

Samples as-treated thermal expansion bars, except † = surface-ground bars, * = sectioned cylinders. crist = cristobalite LZS = lithium zinc silicate

by nucleation at 465 or 585° C (which correspond to regimes of high nucleation rate – see Fig. 3 and discussion). Similar data for composition C are given in Fig. 7b. Also included in Fig. 7b are data for glasses that have not been subjected to a separate sealing cycle; these materials have been given a standard nucleation and crystallization heat-treatment only. The thermal expansion of these materials is less than that of the corresponding glasses that have been subjected to a separate sealing cycle. For both these compositions, thermal expansion generally decreases with increasing crystallization temperature.

3.2. Crystalline phases present

As-cast glasses were fully X-ray amorphous, as were glasses which had undergone nucleation for 1 h at 465° C. Heat-treatment of glasses at > 650° C produced characteristic X-ray peaks which increased in intensity with increasing temperature and time. Some typical X-ray diffraction data are shown in Fig. 8. A number of crystalline phases were identified, including cristobalite, quartz, tridymite and γ_o Li_2ZnSiO_4, as summarized in Table VII. In general, however, the peak positions and corresponding *d*-spacings of the major phase could not be identified positively with any of the known lithium zinc silicate or related compounds, although they were apparently most closely related to the β-lithium zinc silicate series.

Also, as noted in Table VII, differences were found between samples that had been surface ground prior to X-ray examination, and samples that had had no prior surface treatment, suggesting some surface crystallization effects.

3.3. Microstructures

The microstructures of a number of the glass-ceramics are shown in Figs 9 and 10. Fig. 9 shows glass samples that have been nucleated only, at 465 and 585° C, respectively. Fig. 10 shows samples that have also been subjected to a crystallization stage.

3.4. Mechanical properties

Results for the biaxial flexure strength of some of the materials are summarized in Table VIII and Fig. 11. The strongest material studied was composition D, crystallized at a temperature of 750° C, which exhibited a stength of 139 ± 4 MPa.

4. Discussion

The thermal properties of the lithium zinc silicate glasses studied in the present investigation are characterized by two well defined DTA crystallization

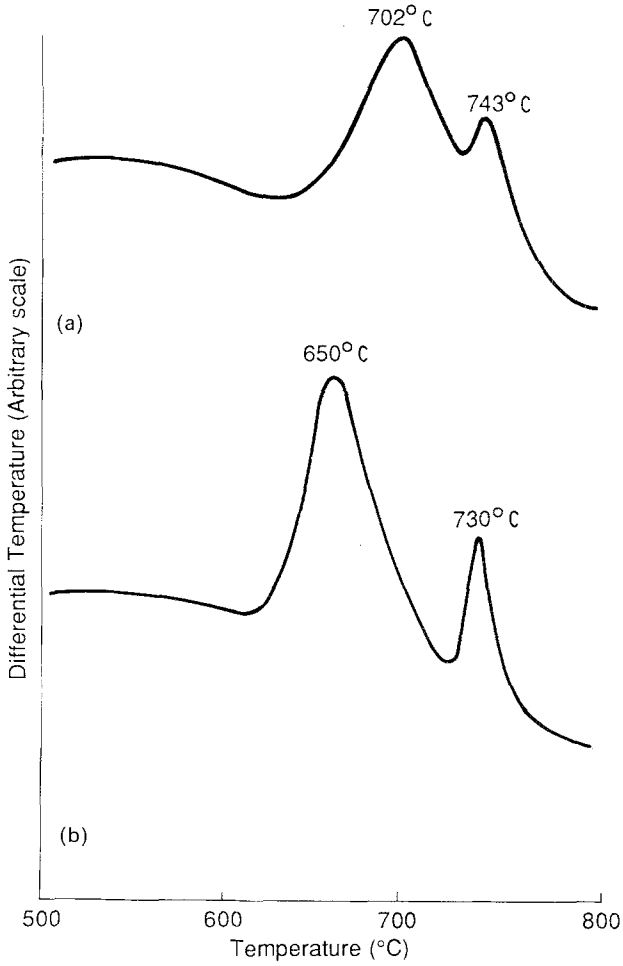

Figure 4 DTA traces of (a) as-quenched and (b) nucleated glass (1 h at 465° C) composition B, illustrating the shift in peak temperatures effected by nucleation.

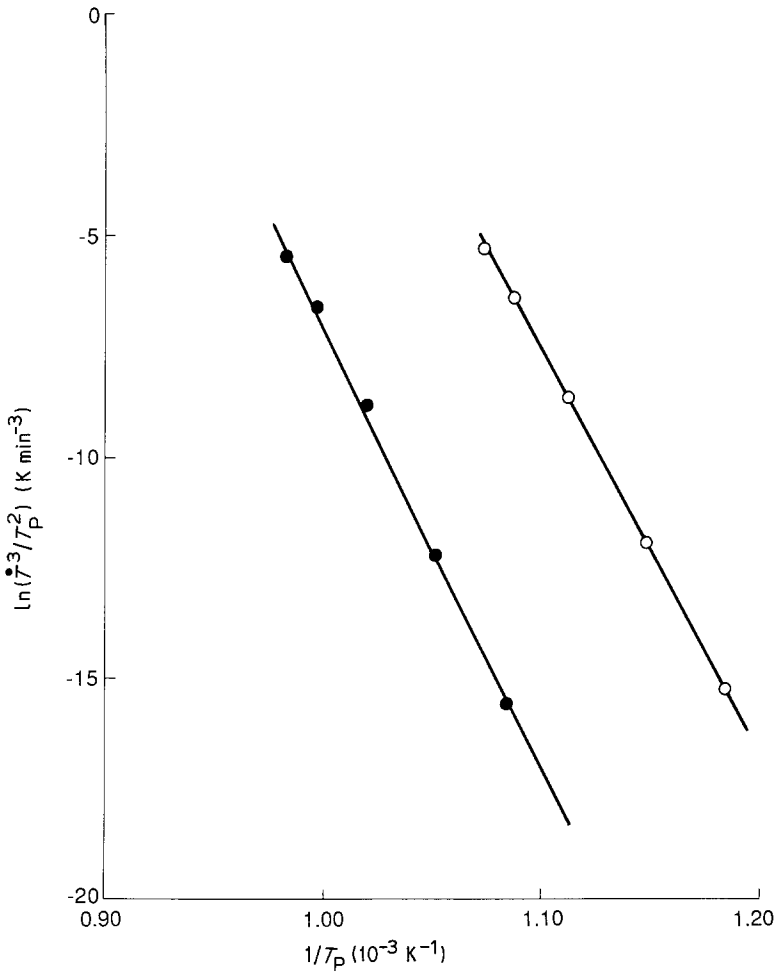

Figure 5 Activation energy plot for glass B. (○ peak 1 = 256 kJ mol^{-1}, ● peak 2 = 280 kJ mol^{-1}).

exotherms, as illustrated in Fig. 2. Of particular interest is the influence of P_2O_5 on the crystallization behaviour of these glasses. The addition of P_2O_5 reduces the temperature of the first crystallization peak as the concentration of P_2O_5 increases from 1.01 to 1.65 mol %, as shown graphically in Fig. 12. There is no significant change in the second crystallization peak over this temperature range.

The simple DTA test for monitoring nucleation efficiency of a given nucleating agent measures the variation in peak temperature with sample particle size. Because the smaller particle size has a larger surface area, the effect of surface crystallization will predominate over bulk crystallization if a nucleating agent is employed that is not very efficient. When an effective nucleating agent is employed, however, there should be little variation in crystallization temperature with particle size. In the present work, the results suggest that the higher concentrations of P_2O_5 act more effectively at promoting bulk crystallization, as summarized in Table V. If, however, the glasses are subjected to a separate nucleation heat-treatment stage prior to crystallization, the lower concentration of P_2O_5 (1.01 mol %) also becomes extremely effective, as summarized in Table V, and illustrated in Fig. 4, which shows DTA traces for as-quenched and nucleated glasses. This result throws doubt on the simple test for assessing the nucleating efficiency, unless a separate nucleation stage is carried out either before or during the test.

In addition to the simple test for monitoring nucleation efficiency using coarse and fine samples of glass, it is also possible to measure the apparent activation energy for crystallization, from which an assessment of the nucleating efficiency can be made. In the present work the Kissinger equation, as modified by Matusita and coworkers [35–37] to take into acccount the crystallization mechanism, was used in this determination. These results, determined for prenucleated samples and summarized in Table VI, show that the lower

TABLE VIII Biaxial flexure strength of glass-ceramics (For glasses nucleated for 1 h at 465° C and crystallized at different temperatures)

Glass code	Temperature of crystallization (° C)	Flexure strength (MPa)
C	glass	91 ± 11
C	700	138 ± 12
C	750	110 ± 13
D	glass	102 ± 10
D	650	92 ± 15
D	700	126 ± 8
D	750	139 ± 4
D	800	133 ± 6
E	glass	79 ± 10
E	700	136 ± 5
E	750	106 ± 8
E	800	113 ± 13
F	glass	85 ± 14
F	650	81 ± 11
F	750	137 ± 2
F	800	118 ± 8

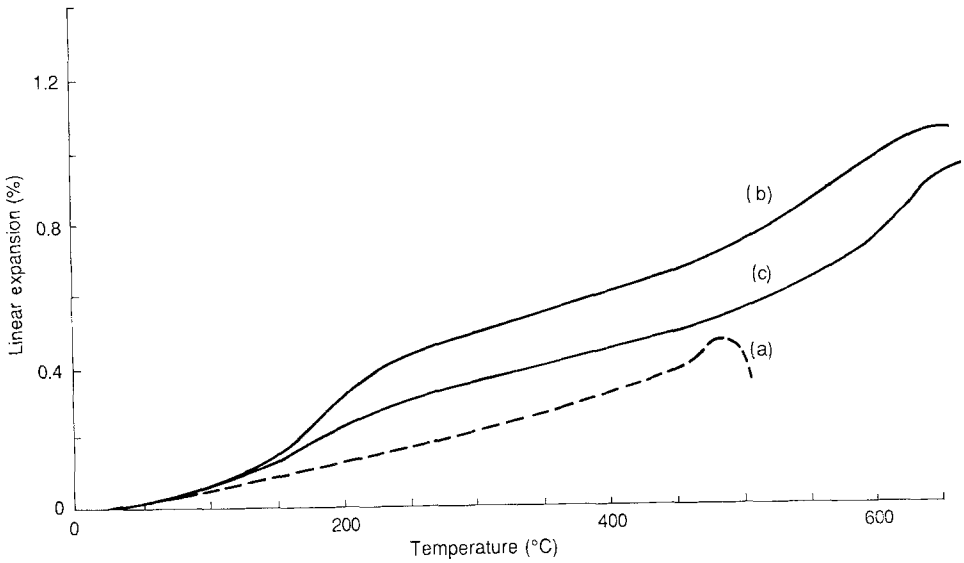

Figure 6 Dilatometer traces for (a) glass and (b and c) glass-ceramics of composition B. Glass-ceramics prepared by nucleating for 1 h at 465° C followed by crystallization for 1 h at, (b) 700° C, and (c) 850° C.

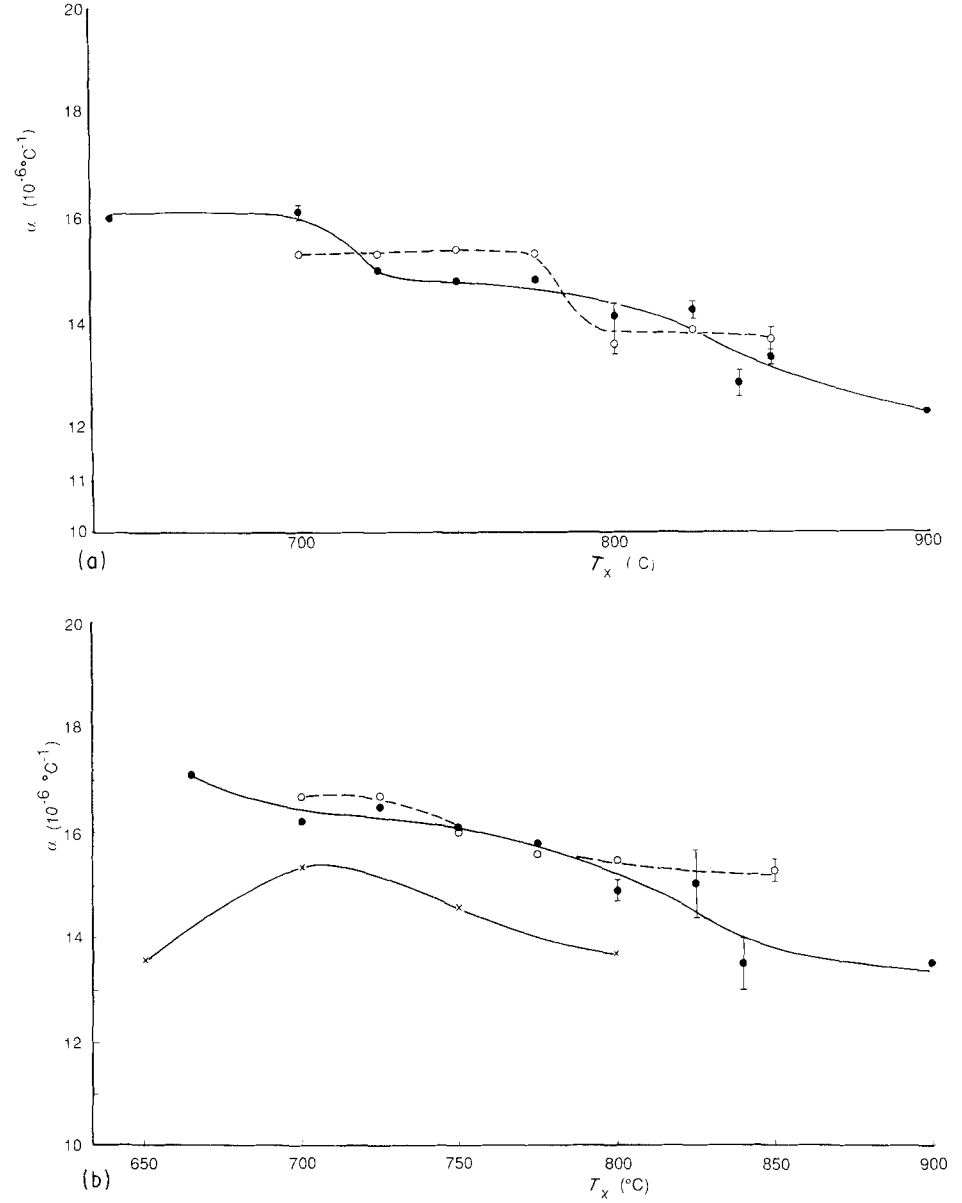

Figure 7 Thermal expansion of glass-ceramics as a function of heat-treatment parameters (20 to 460° C). (a) Composition B. (b) Composition C. (● 950° C/5 min + 465° C/60 min + T_x/60 min, ○ 950° C/5 min + 585° C/60 min + T_x/60 min, × 465° C/60 min + T_x/60 min)

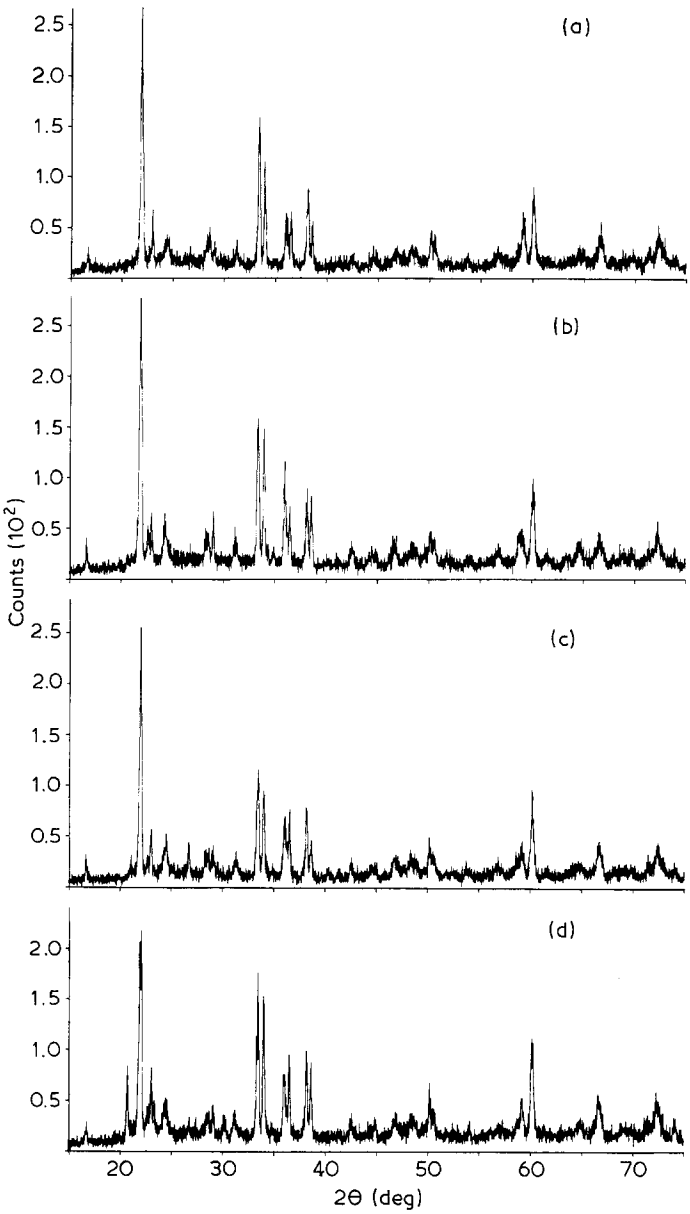

Figure 8 Typical X-ray diffraction traces for lithium zinc silicate glass-ceramic (composition B), crystallized at different temperatures. (a) 700° C, (b) 750° C (c) 800° C, (d) 850° C.

concentration of P_2O_5 gives lower values for the activation energy. This is further evidence in support of our claim that the simple nucleating efficiency test cannot be relied upon to give consistent results, unless the samples are nucleated beforehand.

The optimum nucleating temperatures of the present glasses were determined by the method of Marotta *et al.* [31–34], who have shown that the temperatures determined by their method agree very closely, for a number of glasses, with the optimum temperatures found using more conventional, but more laborious, microscopic techniques. In the present work, we have found an optimum temperature of about 460° C for glass B (Fig. 3a), and ≈470° C for compositions C and D. These results compare extremely favourably with the results of Fairweather *et al.* [28] who employed a direct microscopic technique for determining the nucleation behaviour of a high-ZnO lithium zinc silicate glass. Reference to Fig. 3a of the present work suggests, however, that there is a second higher temperature regime for which high nucleation rates are also obtained (although not as efficient as the lower temperature regime). We postulate that the lower temperature nucleating regime is due to the effect of submicroscopic amorphous phase separation of the glass, whilst the second higher temperature regime is due to the formation of small crystalline nuclei. This is partly supported by microscopic and X-ray evidence. Samples nucleated at 465° C are X-ray amorphous and no detail can be resolved by SEM (Fig. 9a). On the other hand, samples nucleated at 585° C show some crystallinity as resolved by X-ray diffraction, and are composed of relatively small ($< 1\ \mu m$) particles randomly distributed in a glassy matrix (Fig. 9b). Further work is in progress using transmission electron microscopy in an attempt to resolve the structure of the samples that have been nucleated at 465° C.

The microstructures of some samples that have been subjected to nucleation and crystallization stages are shown in Fig. 10. These show that the grain size of the materials increases with increasing crystallization

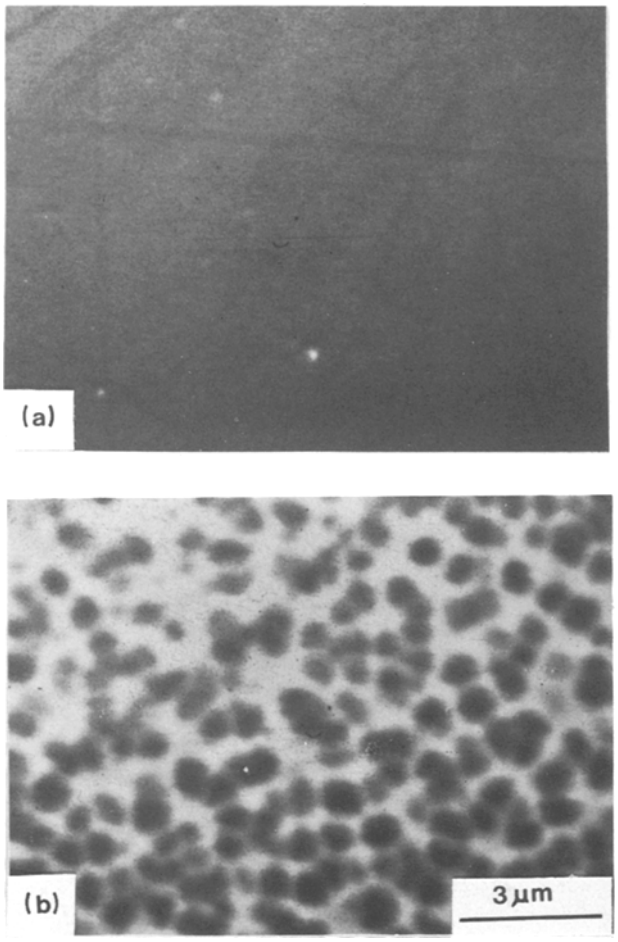

Figure 9 Microstructures of nucleated glasses. (a) Composition C, nucleated at 465° C. (b) Composition C, nucleated at 585° C.

temperature, and this is probably the reason why the mechanical strength of the materials begins to decrease when crystallization is carried out at temperatures greater than 750° C (Table VIII and Fig. 11). The fall in strength from that of the base glass when crystallized at 650° C (Table VIII) is most probably associated with the presence of high internal stresses set up as a result of differences in thermal expansion between the crystalline particles and the glassy matrix. The strength of the materials increases between 650 and 750 ° C as the proportion of residual glassy phase decreases; the strongest glass-ceramics exhibit strengths of between about 36 to 52% greater than that of the base glasses.

The X-ray diffraction data for the present materials are very complex, as summarized in Fig. 8 and Table VII. Cristobalite, quartz and tridymite have been positively identified in some samples, and γ Li_2ZnSiO_4 has been identified in a sectioned bulk sample of glass B crystallized at 850° C. In general, however, the peak positions and associated *d*-spacings of the major crystalline phase do not coincide precisely with any of the reported lithium zinc silicate or related phases; they are apparently most closely related to the β-lithium zinc silicate series. It should be noted, however, that only very limited work has been carried out on the ternary Li_2O–ZnO–SiO_2 system [29, 42–44], and it is far from clear what effect other additions, e.g. B_2O_3, P_2O_5, Na_2O, K_2O or Al_2O_3, will have on the diffraction pattern.

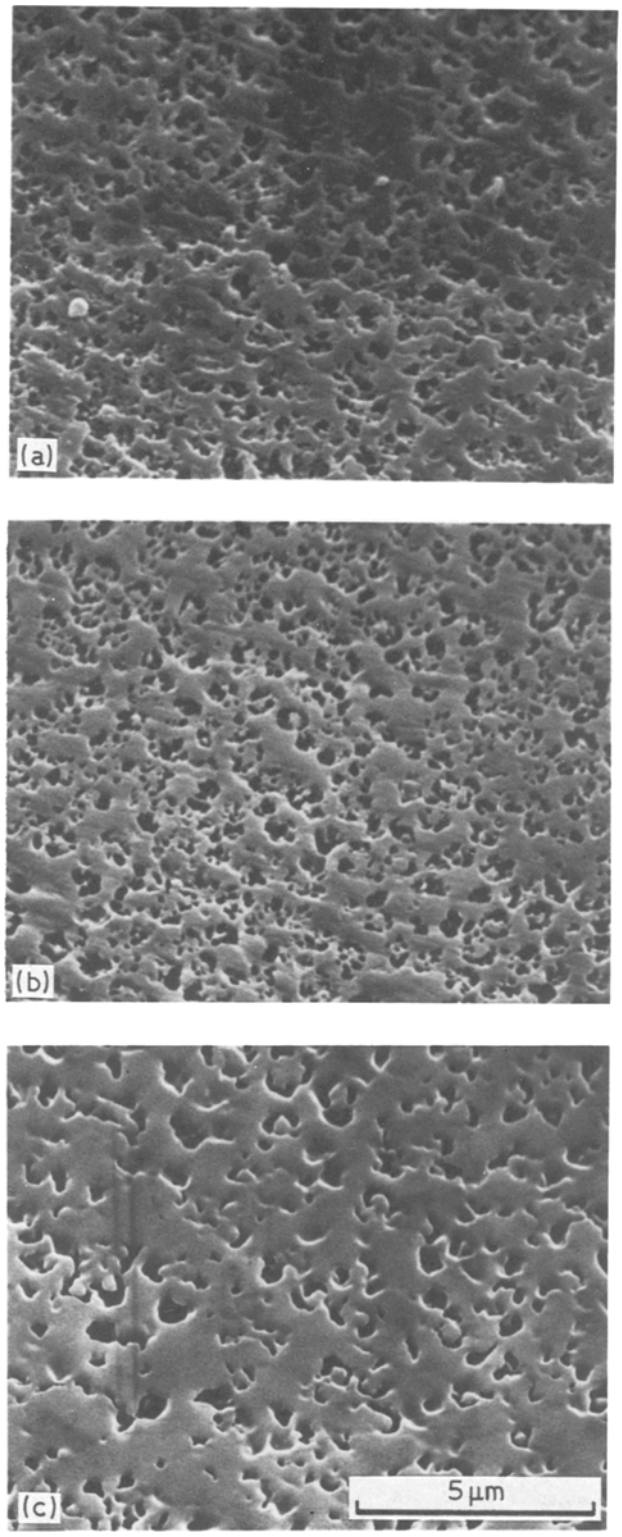

Figure 10 Microstructures of lithium zinc silicate glass-ceramic (composition D) nucleated at 465° C, and crystallized at different temperatures (a) 700° C, (b) 750° C, (c) 800° C.

Reference to the thermal expansion data for compositions B and C (Fig. 7) shows that, in general, the expansion decreases with increasing crystallization temperature in the range 640 to 900° C. This is believed to be due, at least in part, to the replacement of cristobalite by lower expansion quartz and/or tridymite at the higher temperatures. Typical dilatometer traces for the glass-ceramics (Fig. 6) indicate a very pronounced and characteristic α–β cristobalite phase inversion centred around 200° C. This inflection

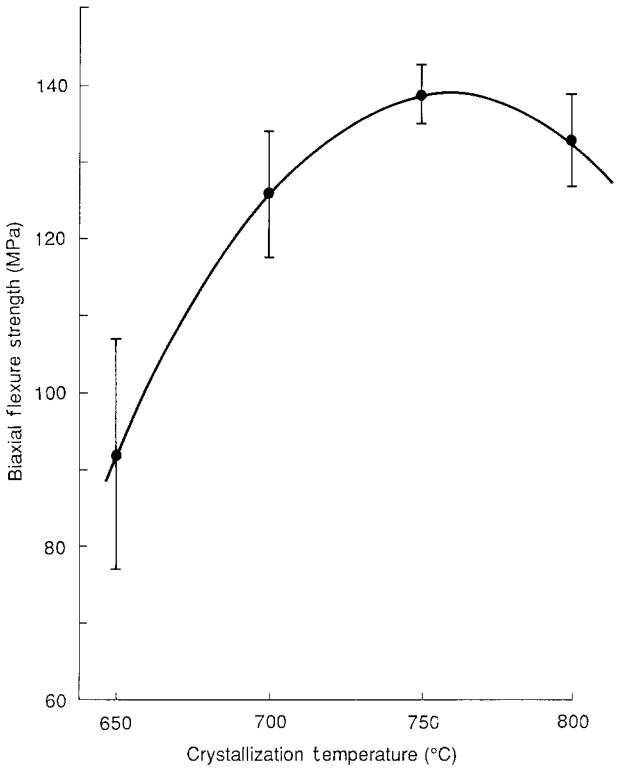

Figure 11 Biaxial flexure strength as a function of crystallization temperature for glass-ceramic of composition D.

becomes less pronounced at higher crystallization temperatures, supporting the view that cristobalite is being replaced by a lower expansion phase. The higher temperature inflection, centred around 520° C is believed to be due either quartz or to a phase change within the major phase which, as already discussed, is most probably some lithium zinc silicate modification. It is noteworthy that the overall expansion of glass B is lower than that of glass C, which has the higher concentration of P_2O_5. Also shown in Fig. 7b are some results for glass C which has been nucleated and crystallized, but has not been subjected to a sealing cycle of 950° C for 5 min (see Fig. 1). The expansions obtained without a simulated sealing cycle are significantly different to those obtained when a sealing cycle is included. This is a very important result. It illustrates clearly the importance, when designing a glass-ceramic material for sealing applications, of employing a full simulated sealing cycle to monitor the change in expansion with heat-treatment parameters.

Work is now continuing employing both high temperature X-ray diffraction techniques and transmission electron microscopy, in an attempt to elucidate in more detail the microstructures and crystal phases formed in this family of lithium zinc silicate glass-ceramic materials. The results of this investigation will be reported at a later date.

5. Conclusions

The conclusions are as follows.

(1) The lithium zinc silicate compositions employed in the present work can be used to prepare moderately high thermal expansion glass-ceramic materials – expansions are in the range of about 12.3 to 17.1 $\times$ 10^{-6} ° C^{-1} (20 to 460° C).

(2) In order to tailor the expansion of these glass-ceramics for sealing applications, it is essential that data are obtained employing a full simulated sealing cycle.

(3) Nucleation and crystallization studies show that the simple nucleating efficiency test, which employs glass powder of coarse and fine particle sizes, can give misleading results unless a separate nucleation stage is carried out either before or during the test.

(4) For the present systems, P_2O_5 is an effective nucleating agent. The optimum concentration is about 1.01 mol %, and the optimum nucleation temperature is about 465° C.

(5) Very complex X-ray diffraction spectra are obtained for the present materials. Cristobalite, quartz and tridymite have been positively identified in some samples. The remaining spectra do not in general coincide precisely with any reported lithium zinc silicate or related phases, although they show some similarity to the β-lithium zinc silicate series.

Acknowledgements

The authors wish to thank Mr I. Jones and Mr M. Clay, AWE, for carrying out the X-ray diffraction work and for interpretation of the data, Mrs M. Porter and Mrs E. A. Prior, AWE, for preparing and examining the samples for electron microscopy, and Dr J. A. Davies, AWE, for chemical analysis of samples. We also are grateful to Sandia National Laboratories,

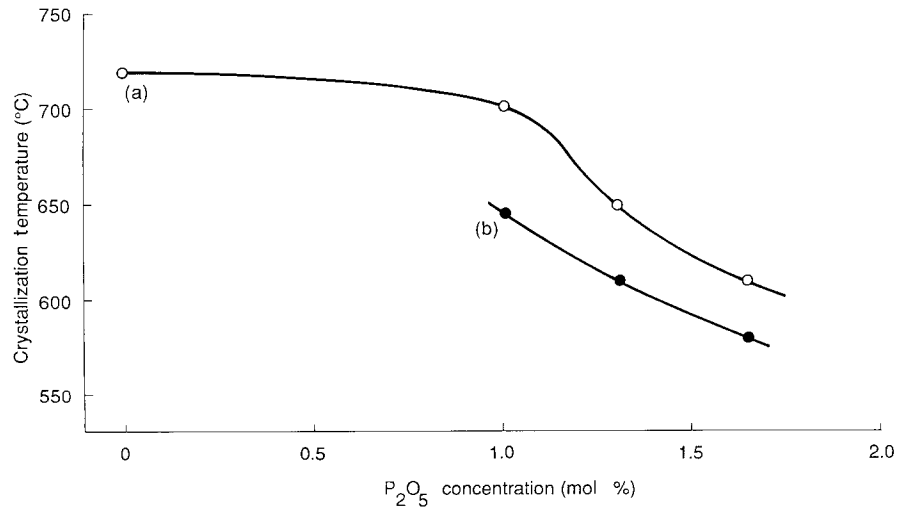

Figure 12 Effect of P_2O_5 concentration on the crystallization temperature of Li_2O–ZnO–SiO_2 glass. (a) as-quenched glass, (b) nucleated glass.

Albuquerque, USA, for supplying some of the glass samples employed in this work.

References

1. J. H. PARTRIDGE, "Glass-to-metal seals" (Society of Glass Technology, Sheffield, 1949).
2. P. W. McMILLAN and B. P. HODGSON, *Engineering* **196** (1963) 366.
3. P. W. McMILLAN, B. P. HODGSON and G. PARTRIDGE, *Glass Technol.* **7** (1966) 121.
4. P. W. McMILLAN, G. PARTRIDGE, B. P. HODGSON and H. R. HEAP, *ibid.* **7** (1966) 128.
5. P. W. McMILLAN, "Glass Ceramics", 2nd edn (Academic Press, London, 1979).
6. M. WADA and S. KAWAMURA, *Bull. Inst. Chem. Res., Kyoto Univ.* **59** (1981) 256.
7. D. G. GROSSMAN, in "Advances in Ceramics 4", edited by J. H. Simmons, D. R. Uhlmann and G. H. Beall (American Ceramic Society, Columbus, OH, 1982) pp. 249-259.
8. G. H. BEALL and D. A DUKE, in "Glass Science and Technology 1", edited by D. R. Uhlmann and N. J. Kreidl (Academic Press, New York, 1983) pp. 241-257.
9. J. HLAVAC, in "The technology of glass and ceramics" (Elsevier, Amsterdam, 1983) pp. 228-243.
10. I. W. DONALD, "Inorganic glasses and glass-ceramics: a review", AWRE Report NO. 0 19/84, 1984 (HMSO, London, 1984).
11. G. H. BEALL, *J. Non-Cryst. Solids* **73** (1985) 413.
12. Z. STRNAD, "Glass-ceramic materials" (Elsevier, Amsterdam, 1986).
13. H. L. McCOLLISTER and S. T. REED, US Patent 441 4282 (1983).
14. T. J. HEADLEY and R. E. LOEHMAN, *J. Amer. Ceram. Soc.*, **67** (1984) 620.
15. D. P. KRAMER and R. T. MASSEY, *Ceram. Engng Sci. Proc.* **5** (1984) 739.
16. G. PARTRIDGE and C. A. ELYARD, *Brit. Ceram. Proc.* **34** (1984) 219.
17. S. G. DZHAVUKTSYAN, *J. Appl. Chem. USSR* **58** (1985) 2440.
18. W. F. HAMMETTER and R. E. LOEHMAN, *J. Amer. Ceram. Soc.* **70** (1987) 577.
19. I. W. DONALD and B. L. METCALFE, AWE, unpublished work (1985-1986).
20. P. W. McMILLAN and G. PARTRIDGE, UK Patent 943 599 (1963).
21. P. W. McMILLAN and B. P. HODGSON, UK Patent 944 571 (1963).
22. P. W. McMILLAN and G. PARTRIDGE, *Proc. Brit. Ceram. Soc.* **3** (1965) 241.
23. P. W. McMILLAN, B. P. HODGSON and G. PARTRIDGE, US Patent 3220 815 (1965).
24. P. W. McMILLAN and G. PARTRIDGE, US Patent 3170 805 (1965).
25. P. W. McMILLAN and B. P. HODGSON, UK Patent 1023 480 (1966).
26. P. W. McMILLAN and B. P. HODGSON, UK Patent 1063 291 (1967).
27. G. PARTRIDGE, S. V. PHILLIPS and J. N. RILEY, *Trans. J. Brit. Ceram. Soc.* **72** (1973) 255.
28. M. J. FAIRWEATHER, J. A. TOPPING and M. K. MURTHY, *J. Amer. Ceram. Soc.* **58** (1975) 260.
29. Z-X CHEN and P. W. McMILLAN, *ibid.* **68** (1985) 220.
30. R. L. THAKUR and S. THIAGARAJAN, *Glass and Ceramic Bull.* **13** (1966) 33.
31. A. MAROTTA, A. BURI and F. BRANDA, *J. Mater. Sci.* **16** (1981) 341.
32. A. MAROTTA, S. SAIELLO, F. BRANDA and A. BURI, *Verres Réfract* **35** (1981) 477.
33. S. SAIELLO, F. BRANDA, A. BURI and A. MAROTTA, *ibid.* **36** (1982) 859.
34. A. MAROTTA, A. BURI, F. BRANDA and S. SAIELLO, in "Advances in Ceramics 4"; edited by J. H. Simmons, D. R. Ulhmann and G. H. Beall (American Ceramic Society, Columbus, OH, 1982) pp. 146-152.
35. K. MATUSITA, S. SAKKA and Y. MATSUI, *J. Mater Sci.* **10** (1975) 961.
36. K. MATUSITA and S. SAKKA, *J. Non-Cryst. Solids,* **38 & 39** (1980) 741.
37. *Idem. Bull. Inst. Chem. Res. Kyoto Univ.* **59** (1981) 159.
38. F. F. VITMAN and V. P. PUKH, *Industrial Laboratory* **29** (1963) 925.
39. J. B. WACHTMAN, W. CAPPS and J MANDREL, *J. of Materials* **7** (1972) 118.
40. ASTM, Standard Test Method for Biaxial Flexure Strength of Ceramic Substrates, ASTM F 394-78 (1978) pp. 802-808 ASTM Committee F-1 (F01.09).
41. J. E. RITTER, K. JAKUS, A. BATAKIS and N. BANDYOPADHAY, *J. Non-Cryst. Solids* **38 & 39** (1980) 419.
42. I. M. STEWART and G. J. P. BUCHI, *Trans. Brit. Ceram. Soc.* **61** (1962) 615.
43. A. R. WEST and F. P. GLASSER, *J. Mater. Sci.* **5** (1970) 557.
44. *Idem., ibid.* **5** (1970) 676.

Received 10 June
and accepted 7 December 1988